INTERNATIONAL JOURNAL OF HYDROGEN ENERGY 45 (2020) 2557–2568

Available online at www.sciencedirect.com

ScienceDirect

journal homepage: www.elsevier.com/locate/he

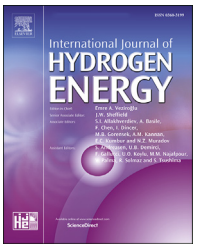

Impact of applied cell voltage on the performance of a microbial electrolysis cell fully catalysed by microorganisms

Swee Su Lim [a,b], *Jean-Marie Fontmorin* [a], *Paniz Izadi* [a], *Wan Ramli Wan Daud* [b], *Keith Scott* [a], *Eileen Hao Yu* [a,*]

[a] *School of Engineering, Newcastle University, Newcastle Upon Tyne, NE1 7RU, United Kingdom*
[b] *Fuel Cell Institute, Universiti Kebangsaan Malaysia, 43600, UKM, Bangi, Malaysia*

HIGHLIGHTS

- Bioelectrodes in the MEC were enriched simultaneously and stable operated over a year.
- The highest hydrogen production (5.9 L H_2/m^2 cathode/day) occurred at 1.0 V.
- PH divergence was inevitable between the chambers and at its maximum after ≥1.0 V.
- High applied voltage (>1.2 V) had adverse effect against bioanode.
- Overall energy efficiency was 29.4% and bioanode provided almost 1/3 of the total energy.

ARTICLE INFO

Article history:
Received 18 September 2019
Received in revised form
29 October 2019
Accepted 18 November 2019
Available online 24 December 2019

Keywords:
Microbial electrolysis cell
Operational applied voltage
Hydrogen production
Bioelectrode development
Bioanode limitation and contribution

ABSTRACT

The effect of the operating voltage on the performance of a microbial electrolysis cell (MEC) equipped with both a bioanode and a biocathode for hydrogen production is reported. Chronoamperometry tests ranged between 0.3 and 2.0 V were carried out after both bioelectrodes were developed. A maximum current density up to 1.6 A m^{-2} was recorded at 1.0 V with hydrogen production rate of nearly 6.0 ± 1.5 L m^{-2} cathode day^{-1}. Trace amounts of methane, acetone and formate were detected in cathode's headspace and catholyte which followed the same trend as hydrogen production rate. Meanwhile substrate consumption in anolyte also followed the trend of hydrogen production and current density changes. The bioanode could utilise up to 95% of acetate in the tested voltage ranges, however, at a cell voltage of 2.0 V the bioanode's activity stopped due to oxygen evolution from water hydrolysis. Cyclic voltammograms revealed that the bioanode activity was vital to maintain the functionality of the whole system. The biocathode relied on the bioanode to maintain its potential during the hydrogen evolution. The overall energy efficiency recovered from both bioanode and external power in terms of hydrogen production at the cathode was determined as 29.4 ± 9.0%, within which substrate oxidation contributed up to nearly 1/3 of the total energy marking the importance of bioanode recovering energy from wastewater to reduce the external power supply.

* *Corresponding author.*
E-mail address: eileen.yu@ncl.ac.uk (E.H. Yu).

https://doi.org/10.1016/j.ijhydene.2019.11.142

Introduction

Bioanodes in bioelectrochemical systems (BES) have been extensively studied and it was reported that negative potentials ranging from −0.28 to −0.41 V vs. Standard Hydrogen Electrode (SHE) could be achieved, depending on the substrates and microbial communities [1–6]. For instance, acetate- and glucose-fed bioanodes can reach −0.22 V and −0.43 V vs. SHE respectively, while open circuit potentials (OCPs) for most bioanodes fed with real wastewaters were reported around −0.33 V vs. SHE [7,8]. In a previous study, we showed that the bioanode is the limiting factor capping the performance of microbial electrolysis cell (MEC) [9]. External energy is needed to drive hydrogen production from water electrolysis in a MEC, and when the applied potential was raised beyond the limit of bioanode, it lost its biotic function to perform substrate oxidation activity. Abiotic oxygen evolution reaction (OER) started to dominate at the anode when bioanode could not provide sufficient electron to the system causing the overshoot of anode potential to more positive [9]. Therefore, it is important to understand the behaviour of bioanode in terms of electrochemical properties and catalytic activities when it is integrated in a MEC alongside with a biocathode.

Up to date, most of the reduction processes involving biocathodes are related with the reduction of CO_2 and proton into desired products such as CH_4, H_2, acetate, formate, ethanol, butanol, etc. [10–14]. Theoretically, the reduction potentials for these products range from −0.24 to −0.41 V vs. SHE. For example, HCO_3^-/CH_4 ($E^{\circ\prime} = -0.24$ V; $8e^-$); H^+/H_2 ($E^{\circ\prime} =$ - 0.41 V; $2e^-$); HCO_3^-/CH_3COOH ($E^{\circ\prime} = -0.28$ V; $8e^-$); HCO_3^-/C_2H_5OH ($E^{\circ\prime} = -0.31$ V; $12e^-$); $HCO_3^-/HCOOH$ ($E^{\circ\prime} =$ - 0.41 V; $2e^-$) in standard conditions of 1 M reactant in water pH 7.0 at 1 atm and 25 °C [8,15,16]. In real conditions, parameters like pH, conductivity and temperature could further increase the potential threshold required to more negative. In the case of protons reduction to hydrogen, the potential varies between 0.00 and −0.83 V depending on the solution pH (H^+/H_2 acidic: 0.00 V; neutral: −0.41 V; alkaline: −0.83 V) causing the increase of the energy input required. Both Rozendal [17] and Jeremiasse [18] regulated pH at neutral in their hydrogen-producing biocathode and managed to reduce proton reduction potential to at least −0.5 V which was determined by chronoamperometry method. Without a stable pH control, the reduction potential could move to more negative than −0.5 V proportionally to the shift of catholyte pH which may require extra input of external power supply [9,10,19].

Theoretically, an external additional voltage of at least 0.13 V is required between the acetate-oxidising bioanode and hydrogen-producing biocathode to drive the oxidation-reduction process in BES. In spite of that, applied voltages higher than 0.5 V were used in most studies considering overpotentials caused by the system and energy losses due to microorganism metabolic activities [18,20,21]. Studies aiming in reducing overpotentials and cutting down operation cost and development time have been carried out [8,22,23]. Nevertheless, some answers still remain elusive when both bioanode and biocathode are operated in the same system. In order to fully understand and control these systems, better understanding of optimum operational environments for bioelectrodes (e.g. pH, conductivity, cell voltage), time of growth for both bioanode and biocathode (e.g. 1 vs. 4 weeks), optimum reducing power or potential required by biocathodes to produce certain products (e.g. HCO_3^-/CH_3COO^- $E^{\circ\prime} =$ -0.28 V vs. H^+/H^2 $E^{\circ\prime} =$ -0.41 V) when coupled with bioanode for wastewater treatment and most importantly interaction of bioanode and biocathode in a single cell system (e.g. current response and how biofilms evolve) even during the beginning of the enrichments is still needed.

A MEC fully catalysed by microorganisms for the purpose of hydrogen production and wastewater treatment was demonstrated by Jeremiasse [18] for the first time. Although the current density increased during enrichment and maintained at significant level (1.9–3.3 A m^{-2}), the whole system still suffered from a low hydrogen recovery at the cathode (17–21%) for a cathode potential of −0.7 V (pH on anode and cathode were controlled at 7.0). The authors also reported other limitations in the system including the precipitation of calcium phosphate on the cathode's surface blocking hydrogen evolution under low reduction potential and methanogen contamination after long term operation. However, no further study was conducted to overcome these issues. Kumar [24] discussed the efficiency of biocathode hydrogen production through a start-up viewpoint. In the review, they surveyed the main influencing factors and methods from literature included the selection of inocula, bioelectrode enrichment and acclimation, operating conditions and cell architectures. They concluded that proper start-up factors and methods are the keys for long-term viability and effectiveness of a MEC fully catalysed by microorganisms. In fact, the usage of microorganisms as biocatalyst in the system can reduce the cost of investment because they can multiple as long as the environment favours the growth. Similar to the MEC system mentioned above, Coma [25] and Luo [26], in different studies, showed that sulphate-reducing biocathode can be enriched and acclimatised simultaneously with a electricity-generating bioanode in a single BES for the purpose of sulphate removal. In Coma [25]'s results, the interaction of the bioelectrodes and their potentials and electrolyte evolvements based on applied voltage were presented. They also found that the anode potential was gradually increasing throughout the study with no substrate oxidation at the anode. The phenomenon was most likely caused by a weak bioanode and the entire anode reaction was dominated by abiotic OER instead of electroactive microorganisms. Meanwhile, Luo [26] improved the system by imposing pH control and feeding mode in cathode. Even though the sulphate removal increased, the contribution of bioanode to the whole system was not studied. Nevertheless, both studies presented by Coma [25] and Luo [26] were focused on sulphate removal and not hydrogen production in the cathode.

The aim of this experiment is to study the interactions between the electricity-generating bioanode and hydrogen-producing biocathode under a range of applied cell voltages. The evolution of the bioelectrodes during the enrichment process and chronoamperometry tests were observed. In addition, effluents from each tests were collected and analysed to support the study. At the end of the study, energy

recovery and contribution between bioelectrodes and power supply for hydrogen production were determined.

Materials and methods

Cell setup, enrichment and operation

Two-chamber MECs were assembled according to Lim [9] with plain graphite felt as both anode and cathode unless stated otherwise. Inoculum for both anode and cathode was collected from a parent microbial fuel cell fed with glucose and glutamic acid and operated over a year. The community of the inoculum was previously determined and shown to be dominated by *Geobacter* sp. [4]. Anodic medium consisted of 50 mM mono- and di-sodium phosphate buffer (PBS) pH 7.0, 10 mM sodium acetate, 5 mM ammonium chloride, 10 mL trace minerals and 10 mL vitamins, as reported elsewhere [9] while cathodic medium contained 50 mM PBS, 10 mM $KHCO_3$, 5 mM ammonium chloride, 3 mM magnesium sulphate and 1 mL trace element mixtures [17]. The media were purged with 99.999% N_2 for 15 min before being injected into each chamber with inoculum in a ratio of 1:1. The cells were left overnight before a constant cell voltage of 0.3 V was applied between anode and cathode. The applied voltage was chosen as acetate-fed bioanode was used in this study. The lowest potential that most acetate-fed bioanode can reach is around −0.22 V compared to standard reduction potential of acetate which is −0.28 V [9,27]. Such bioanodes are commonly used in laboratory conditions because of their stable and consistent current generation. In order to couple bioanodes and biocathodes reactions into a single cell, a minimum external power supply of [X - (−0.22)] V is required, where X is the reduction potential of desired product. In this study, the objective is to develop a hydrogen-producing biocathode [H_2/H^+ $E^{o'} = -0.41$ V] at neutral pH. According to the considerations explained above, the minimum theoretical applied cell voltage was determined as 0.19 V but 0.30 V was chosen as a starting potential to take into account the energy losses and overpotentials at both electrodes. The media of both anode and cathode were replaced when the current of the cells dropped to less than 10% of peak current. Once the bioelectrodes were developed, the feed of anode was changed from batch to fed-batch mode using pre-set on-off timer (Electric Timer Switch ETU17, Timeguard, UK) and a peristaltic pump (Watson Marlow 120U/DM3, UK). The timer was set 'on' for 10min for every 6 h gap and the peristatic pump was set at flowrate of 3 mL min^{-1} unless stated otherwise. Experiments were carried out in duplicates. The rest of the operational conditions are summarised in Supplementary data: Table S1.

Electrochemical methods

Potential monitoring: A multichannel data logger (NI-USB-6225, National Instruments, UK) was used to monitor the cell and electrode potentials throughout the experiments. Cell voltage was measured between anode and cathode while half-cell potentials were measured between the anode or cathode and reference electrodes (RE-5B Ag/AgCl, BASi, USA) located in the corresponding chamber. All potential values except applied cell voltage were reported vs. SHE unless stated otherwise.

Electrochemical impedance spectroscopy (EIS): A potentiostat (PGSTAT128N, Metrohm, Netherlands) equipped with FRA32M module was used for this analysis. Four spectrograms were recorded for each cell; (a) cathode-anode, (b) cathode only, (c) anode only and (d) membrane only. The sum of internal resistances (b) + (c) + (d) should be equal to the value from (a). Analysis frequencies were ranged from 100.000 to 0.01 Hz at open circuit potential.

Cyclic voltammetry (CV): A multichannel potentiostat (Quad, Whistonbrook Technologies, UK) was used to perform the cyclic voltammetry. Voltammograms were taken for both anode and cathode in order to assess their catalytic activity. Cathode was scanned from 0 to −1.0 V vs. SHE and anode from −0.6 to +0.4 V vs. SHE. At least two cycles were recorded and the second cycles are presented in the results. All CVs were performed at scan rate of 0.001 V s^{-1}.

Chronoamperometry (CA): The same potentiostat (Quad, Whistonbrook Technologies, UK) was used to control the cell voltage during the chronoamperometry experiments. A fixed voltage of 0.3 V was applied during the enrichment process unless stated otherwise. CA tests were performed to determine the performance of bioelectrodes especially in biocathode in terms of soluble organic matters and hydrogen generation. Ranging from 0.3 V to 2.0 V, the cell voltage was applied for two days before changing to another applied voltage in an increment order of 0.1 or 0.2 V.

Analytical methods

pH and conductivity: pH and conductivity were measured using a portable pH meter (HI9025 microcomputer pH meter, Hanna Instruments, UK) and conductivity meter (HI 8733, Hanna Instrument, UK), respectively. All samples were filtered through 0.2 μm syringe filters to remove suspended solid and biomass before measurements.

Total organic/inorganic carbons (TOC): A total carbon analyser (TOC-5050A, Shimadzu, UK) equipped with an autosampler (ASI-5000A, Shimadzu, UK) was used for this analysis. At least 5 mL were sampled and filtered on 0.2 μm syringe filters. Total organic compounds concentration were described as organic carbon concentration relatively to carbon dioxide. All values were reported in mg HCO_3^- equivalent L^{-1}. Considering that the mineralisation of 1 mol of acetate produces 2 mol of carbon dioxide, 1 g per litre sodium acetate will produce about 1.073 g CO_2 L^{-1}. Results were cross checked with acetate concentration quantified by gas chromatography and found consistent within 10% error.

Short-chain fatty acids (SCFA): The presence of fatty acids was analysed using a gas chromatography (Tracera GC-2010 Plus, Shimadzu, UK) equipped with Barrier Ionization Discharge (BID) detector (280 °C) and autosampler (AOC-20i, Shimadzu, UK). A column (Zebron ZB-WAX-Plus capillary column 30 m × 0.25 mm × 0.25 μm, Phenomenex, UK) was used to separate the compounds and operated with a temperature profile of 50 °C for 1 min to 180 °C at 30 °C min^{-1} to 180 °C for 8 min. The injection port was set at 180 °C with split ratio 10:1 under 1.0 μL injection sample while the detector was maintained at 280 °C. The carrier gas was high purity grade

helium (99.999% BOC, UK) and was maintained at constant flow 2.0 mL min^{-1}. All samples were filtered with 0.2 μm syringe filters and then acidified with HCl 1.0M with ratio of 9:1 prior analysis.

Energy recovery

The energy produced by the bioanode and consumed by the biocathode was calculated to evaluate the overall efficiency of the system studied. The energy recovery and efficiency were determined based on acetate as the sole carbon source at the anode and hydrogen as the main product at the cathode. The efficiency of the hydrogen recovery from cathode, r_{cat} was determined based on Faraday's law of electrolysis process as:

$$r_{cat}(\%) = Q_{recovery} \Big/ Q_t \times 100\% \quad (1)$$

where $Q_{recovery}$ (C) $= \eta \cdot F \cdot z$ is the charge consumed to reduce protons to hydrogen, η is hydrogen produced in mole, F is Faraday constant (96485 C mol^{-1}), z is the valency number of hydrogen formation which is 2 [$2H^+ + 2e^- \rightarrow H_2$]. Meanwhile, Q_t (C) $= \int I\,(t)\,dt$ is total charge supplied from the power supply and anode, or in other term total charge transferred between anode and cathode.

Meanwhile anodic columbic efficiency was obtained according to [28]:

$$r_{CE}(\%) = Q_t / Q_{oxidise} \times 100\% \quad (2)$$

where $Q_{oxidise}$ is charge produced from substrate oxidation (C) which is equalled to $S \cdot b \cdot F \cdot V_r$, S is substrate consumed (mol L^{-1}), b is stoichiometric number of electron produced per mole of acetate oxidised which is 8 [$CH_3COOH + 2H_2O \rightarrow 2CO_2 + 8H^+$], F is Faraday constant (96485 C mol^{-1}) and V_r is anodic reactor volume (0.025 L).

The overall energy efficiency η_{e+s} of the system is calculated based on [29]:

$$\eta_{e+s}(\%) = W_h / (W_e + W_s) \times 100\% \quad (3)$$

where W_h, W_e, and W_s (J) are the energy contents of hydrogen, supplied electrical energy and energy released from substrate oxidation, respectively. The standard enthalpy of combustion for hydrogen and acetate are 285.83 kJ mol^{-1} and 870.28 kJ mol^{-1}, respectively. Therefore, W_h and W_s were calculated by multiplying the enthalpy values with total moles of hydrogen produced and acetate consumed. Meanwhile, W_e was computed by multiplying the applied voltage value with the total charge flow between the anode and cathode which is also equalled to Q_t.

The energy yield relative to the electrical input can be expressed as follows:

$$\eta_e(\%) = W_h / W_e \times 100\% \quad (4)$$

and the energy yield relative to the substrate oxidation (acetate) is:

$$\eta_s(\%) = W_h / W_s \times 100\% \quad (5)$$

The energy contribution by external power input (e_e) and substrate (e_s) in the system at specific applied voltage were calculated as

$$e_e = W_e / (W_e + W_s) \times 100\% \quad (6)$$

$$e_s = W_s / (W_e + W_s) \times 100\% \quad (7)$$

Results and discussion

Enrichment and operation of bioelectrodes

Both bioanodes and biocathodes were enriched simultaneously at a fix cell potential of 0.30 V after being left for four days at OCP. Fig. 1 (a1), (a2) and (a3) shows the potential profiles of anode and cathode during the enrichment period as well as the current density profile in (b1), (b2) and (b3). As can be seen in Fig. 1 (a1), the anode potential was about +0.20 V when 0.30 V was first applied (4.6 days) before starting to decrease within a day to −0.10 V (7.4 days) and reaching nearly −0.48 V after the medium was replaced for the second time (8.3 days). On the other hand, the current density increased within 10 days of operation, confirming the growth of the bioanode. Meanwhile, the cathode potential followed the trend of the anode, reaching −0.76 V after the second cycle. The bioanode developed quicker and dragged the cathode potential down to more negative. This lower potential created more suitable conditions for the biocathode development which in turn favoured protons and CO_2 reduction. After then, both anode and cathode media were changed according to the bioanode cycle, i.e. every 3–4 days. It is believed that anode reaction was faster than cathode reaction as substrate is being oxidised at the anode, in opposition to products being generated at the cathode (e.g. fatty acids and hydrogen in this case) [12,13,30,31]. A further small drop of cathode potential was observed at 60 days (Fig. 1 (a1)) but no significant current increased until 130 days (Fig. 1 (b1)). This increase was most likely associated with the biocathode enrichment which requires longer time to enrich than the bioanode [13,31].

Chronoamperometry test and hydrogen production

In order to understand the behaviour of each electrode and their interaction at different applied cell voltages, the cells were subjected to a range of voltage from 0.3 to 2.0 V with tested period of two days for each voltage between 286 and 319 days [13,31]. Fig. 2 shows the monitored voltage, potentials and current densities during the chronoamperometry experiments summarised in Supplementary data: Table S1, whereas Fig. 3 shows the corresponding hydrogen and other organics production rates in the cathodic compartment. Both the oxidation of acetate at the anode and the hydrogen production at the cathode started when the applied voltage reached 0.7 V, as shown in Figs. 2 and 3. Above 0.7 V, the cathode potential was more positive than −1.0 V, thus not low enough to support the hydrogen production of hydrogen. In previous studies, convincing evidences showed that the hydrogen production in this system was a combination of biotic and abiotic proton reduction activities [9,21]. Biotic hydrogen production rate prevailed and increased significantly when the cathode potential was set at −0.8 V and below. The cell voltage was around 0.6 V before it started to increase as compared to a control (without added inoculum).

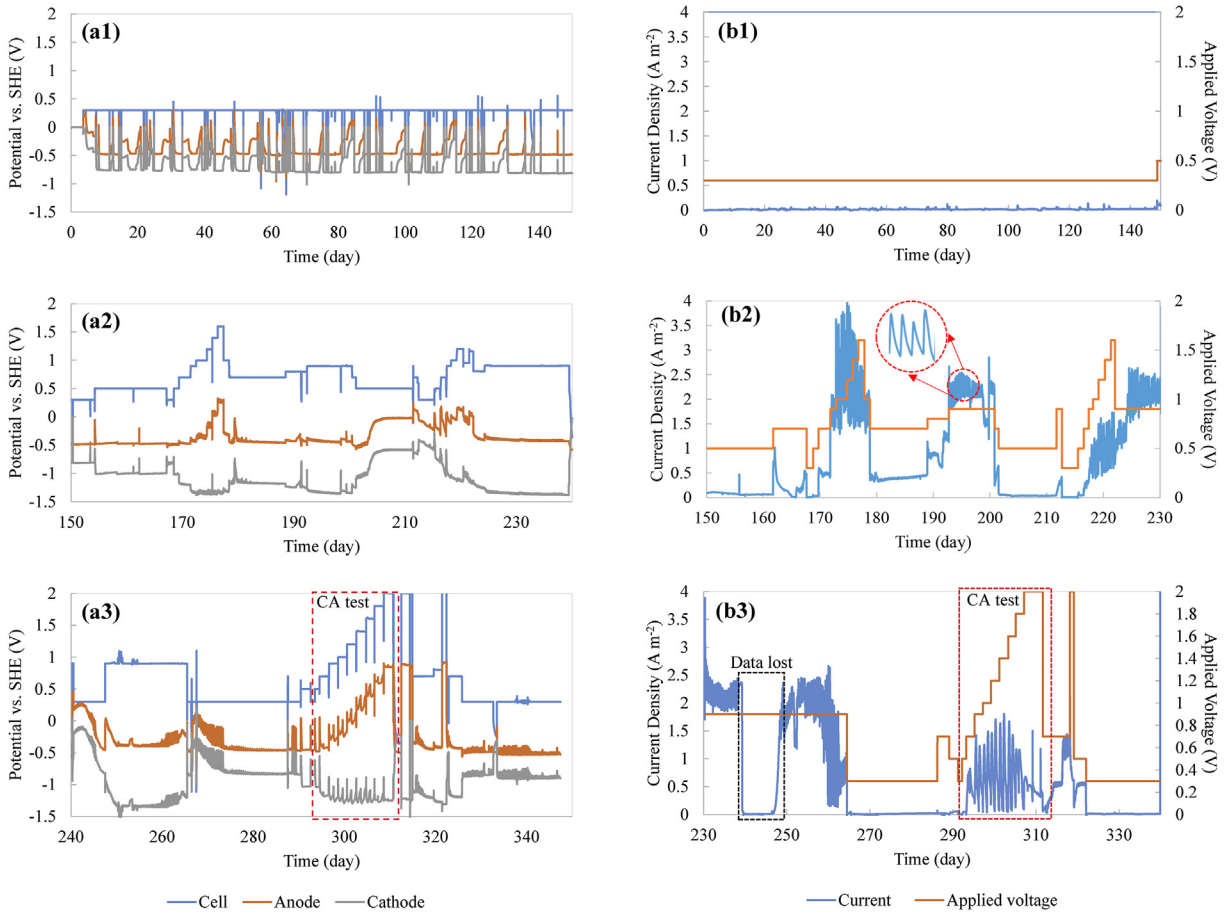

Fig. 1 – The profile of (a) electrode potentials and (b) current density for the microbial electrolysis cell with functional bioelectrodes. Data for (a1) and (b1) were collected during the enrichment step at 0.3 V while (a2), (b2), (a3) and (b3) consist of several tests including chronoamperometry tests (sequential order of applied voltages) with the applied voltages ranging between 0.3 and 2.0 V. Note: the noise noticeable in the figures especially for the current density is due to the cell cycles when substrate is depleted and medium is replaced (See the zoom-in profile in (b2)).

It is fair to infer in this study with the same setup similar activities occurred in the so called "biocathode" increasing the total hydrogen production ability. Below these applied voltages, excess electrons were accumulated in bioanode instead of being used in biocathode. These observations are consistent with the very low H_2 concentration measured in the headspace for applied potentials below 0.7 V (Fig. 3 (a)). At 0.7 V and above, the oxidation potential at the anode increased thus inducing the reduction of protons and CO_2 at the cathode by supplying more electrons. At this point, the cathode potential reached almost −1.0 V with the lowest potential recorded as −1.1 V. It is believed that pH variation affected the cathode potential and performance, as will be discussed in the next section 'Section Electrolyte properties: electrolyte properties'.

Due to the faster growth of bioanode than biocathode (days vs. weeks) and microbiological characteristics (organotrophs vs. chemoautotrophs) [5,11,13,31–33], the catholyte was replaced after two feed cycles of bioanode. Since then the bioanode potential kept evolving and increasing according to its feed cycles at higher applied voltages. In contrast, for cell voltages higher than 0.7 V, the biocathode potential reached about −1.1 V and remained fairly constant until the end of the experiment. As shown in Fig. 3 (a), a cell voltage of 1.0 V (corresponding cathode potential −1.1 V) appeared as optimal considering the volume of hydrogen measured, which was also consistent with other studies [9,10,17,21,31]. The test was carried out until the bioanode failed to oxidise substrate and produce electrons, which occurred at applied voltage of 2.0 V, where a decrease in current density, lower hydrogen production and acetate removal rates were observed (see 'Section Bioelectrode limitation at high applied voltage: *Bioelectrode limitation at high applied voltage*'). It can be assumed that the higher oxidation potential induced abiotic reactions especially oxygen evolution harming the anaerobic bioanode [9].

These results show that for cell voltages lower than 2.0 V, the role and performance of the bioanode are critical for the viability of the whole system. Indeed, as the catalytic activity of the bioanode collapses, the hydrogen generation rate drops. Although the cathode potential remained constant, the loss of the biocatalytic activity at the anode resulted in a lower current density. The current density profile in Fig. 2 (b) indicates the rate of electrochemical reactions in the system where the optimised applied voltage should lay in between 0.7 and 1.8 V.

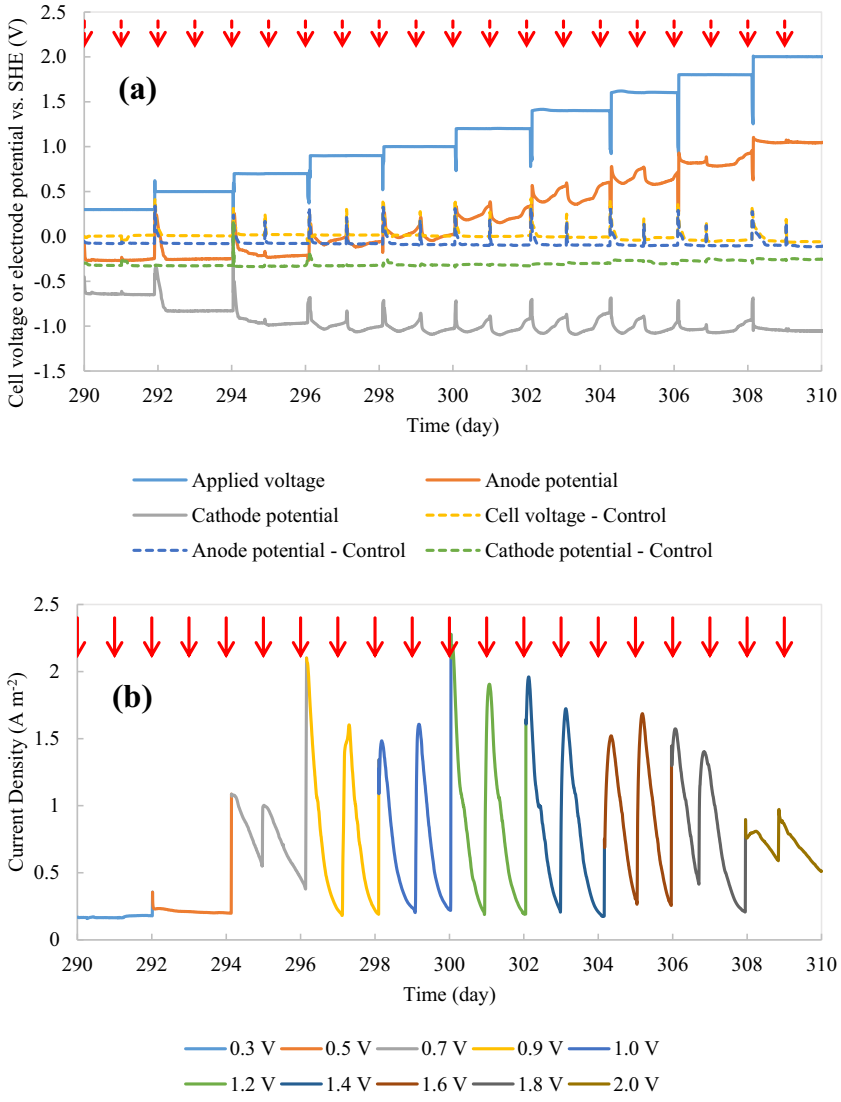

Fig. 2 – (a) Applied voltage and electrode potential profiles and (b) current density of external power supply to the cells during the chronoamperometry test.

Further investigation on the hydrogen evolution rate in Fig. 3 (a) narrowed down the applied voltage to a range from 0.9 to 1.2 V with a maximum hydrogen production rate measured at 1.0 V.

Fig. 3 (b) and (c) presents the total organic/inorganic carbon concentrations in anode and cathode effluents and the organic compounds measured in the catholyte at the end of each chronoamperometry test. Sodium acetate was added into the anolyte as the main carbon source for electrochemically-active microbes to conserve energy and produce electrons. At the beginning of the enrichment, the anolyte and catholyte were replaced according to the cell current density and potential of the anode. As total organic carbon concentration (<5.0 mg L^{-1}) and hydrogen production were negligible in the cathode compartment, the catholyte was eventually replaced according to every two to four anode cycles before starting the chronoamperometry experiments. The aim is to increase the accumulation of trace amount of CO_2-reduced compounds such as acetate which in turn provides better condition for hydrogen-producing bacteria to grow during the start-up period [34,35]. At the end of each cycle, effluents were collected and analysed to identify the total carbon (TC) in the form of carbon dioxide equivalent (Fig. 3 (c)) and content of volatile fatty acids (VFAs) (Fig. 3 (d)). VFAs have been reported in biocathode studies including acetate (C2) and butyrate (C4) [13,15]. Recently, even longer chain fatty acids and alcohols such as caproate (C6) and butanol (C4) were synthesised from a biocathode [11,12,14]. However, the production of such carbon compounds require longer time of operation, low potential (<-0.85 V vs. SHE) and low pH control (5.8) conditions in order to accumulate the desired products up to significant concentrations (e.g. 0.55 g nC6 L^{-1} day^{-1} [11]).

As shown in Fig. 3 (b), the organic carbon removal (or acetate consumption) was consistent with hydrogen production, pH and conductivity value shifts except at 2.0 V applied voltage. At the anode, the result caused the potential shifted

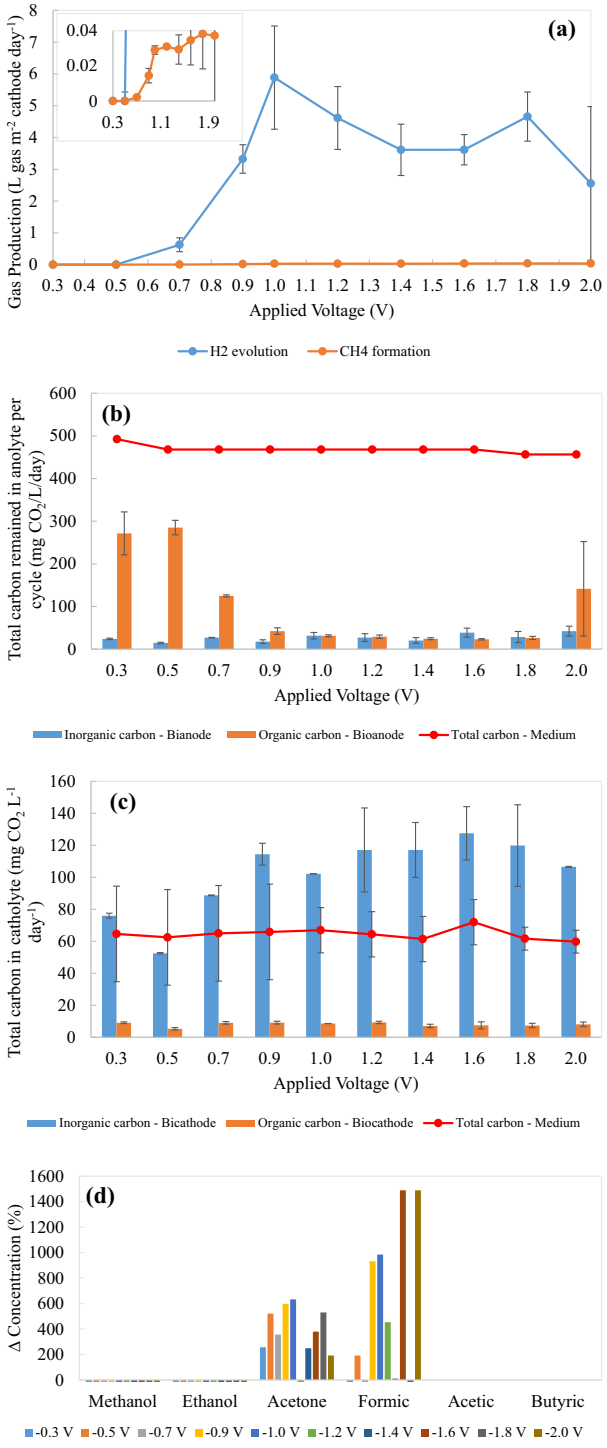

Fig. 3 – (a) Hydrogen evolution and methane formation. Total organic/inorganic carbon: (b) remained in anolyte, (c) accumulated in catholyte, and (d) percentage of difference in organic carbons by compared to control from the chronoamperometry test.

more positive in order to increase acetate oxidation and electron supply [9]. However, as discussed above, the biotic oxidation of acetate significantly dropped at 2.0 V applied voltage when the anode potential exceeded +1.0 V vs. SHE, which was characterised by the accumulation of organic carbon in the anolyte, as depicted in Fig. 3 (b). The organic carbon in fresh anode medium was higher at the beginning due to the added acetate, low concentration of organic and inorganic carbons was detected in the effluent of the anode. Small amount of CO_2 was generated through the oxidation of acetate contributing to the inorganic value in the effluents [33].

The accumulation of organic carbon in the catholyte was low (10 mg CO_2 L^{-1}) compared to inorganic carbon concentration but higher than in the control effluent sampled at the same time (by 10–30%, data not shown). The low concentrations measured can be associated with the slow kinetics of formation of organic carbon-based compounds at the cathode and slow development of the biocathodes which typically require weeks or months under low poised potentials [11–13,30–32,36]. In addition, cell voltages were only applied for two days, which did not allow the accumulation of significant amounts of organic compounds in this experiment. The accumulation of hydrogen in the cathode environment could trigger the growth of methanogens which in turn produce methane and reduce hydrogen yield [21,30,37]. This phenomenon was somehow noticed in Fig. 3 (a), although methane concentrations detected in this experiment were

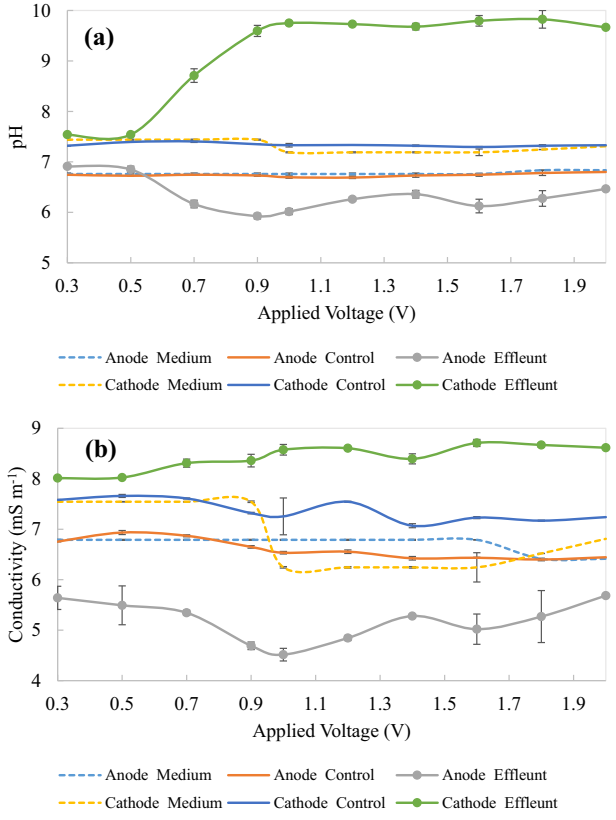

Fig. 4 – The profiles of (a) pH and (b) conductivity in anode medium and catholyte relatively to various applied voltages. Note: All lines marked with medium and control are not subjected to chronoamperometry test. The samples were collected at the same time with effluents at specific applied voltages during the test. They are shown for comparison.

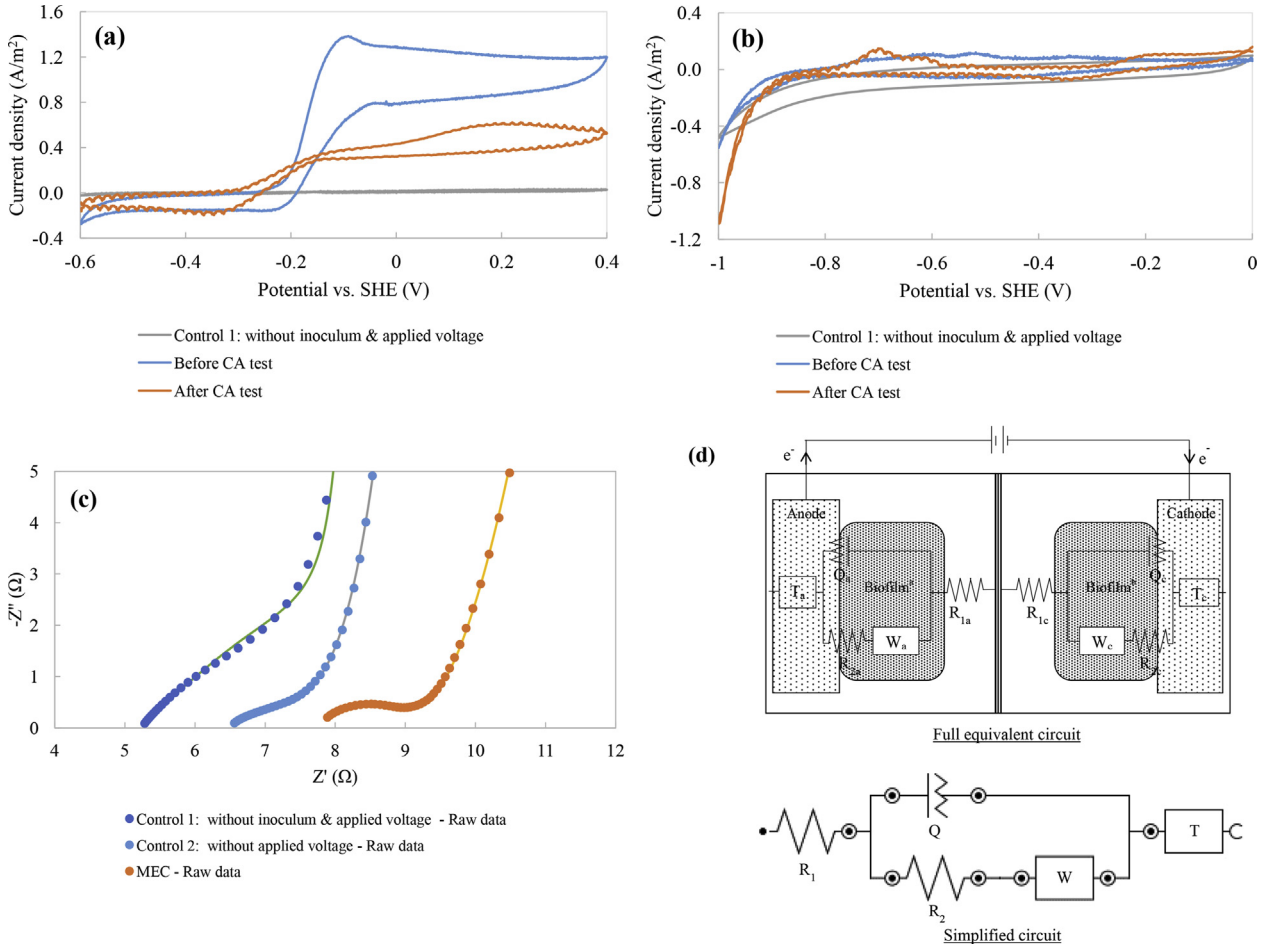

Fig. 5 – Cyclic voltammograms of the bioanode and biocathode in bioelectrochemical cells (a) anodic, (b) cathodic catalytic activities and electrochemical impedance spectrograms: (c) Nyquist plot, and (d) equivalent circuit with its simplified version: [R_1(Q[R_2W])T] where R_1 = solution resistance, R_2 = charge transfer resistance, Q = constant phase element, W = Warburg diffusion element, and T = finite diffusion element.

very low (about 0.04 L CH_4 m^{-2} day^{-1}). In comparison with anode effluents, the trend of organic carbon of cathode showed almost the same values across the applied voltages with slightly higher than control (without applied voltage, data not shown). However, inorganic carbon in the form of carbonates appeared significantly in cathode effluent indicating the carbonates (produced from acetate oxidation) diffused through membrane from the anodic chamber and accumulated in the catholyte as presented in Fig. 3 (b) and (c). Concentration differential and pH gradient (See Section Electrolyte properties: Fig. 4 (a)) between the chambers triggered the migration of the carbonates into cathodic chamber.

Electrolyte properties

Fig. 4 displays the profile of pH and conductivity of the anodic and cathodic effluents based on applied voltages. Media used in the tests and control cell have been included in the same figure to facilitate comparisons. No significant change in pH and conductivity was observed for applied cell voltages between 0.3 and 0.5 V. The pH and conductivity values remained unchanged around 7.0 and 7.0 mS m^{-1}, respectively. However a significant shift of conductivity in anode and cathode effluents from 7.0 to nearly 8.0 and 6.5 mS m^{-1} were measured at applied potential of 0.3 V, respectively. At applied potentials of 0.5 V and higher, the pH and conductivity of anodic effluents decreased from 7.0 to 6.0 and 6.0 to 5.0 mS m^{-1} respectively and remained constant after 0.7 V. On the other hand, the pH and conductivity of cathodic effluents increased from 7.0 to 9.7 and 8.0 to 8.5 mS m^{-1}, respectively between 0.5 and 1.0 V. The pH and conductivity values remained plateau after 1.0 V and above. In summary, the pH of anode decreased due to acetate oxidation process releasing protons in to the solution [2,4,38]. The reduction of substrate to low weight compounds also reduce the ionic strength of the solution causing the conductivity to fall. Meanwhile, the cathode pH increased as protons were constantly removed from the solution to form hydrogen [18,34]. Therefore, the conductivity value increased at higher applied voltages.

Bioelectrode limitation at high applied voltage

After chronoamperometry at 2.0 V, cyclic voltammograms and electrochemical impedance were recorded for the anode

Table 1 – Coefficient values determined from the equivalent circuit in Fig. 5 (d).

Cell	Solution resistance		Constant phase				Charge transfer resistance		Semi (Warburg)-diffusion		Finite diffusion				Internal Resistance	
			Impedance		Element constant				Impedance		Impedance		Time constant			
	R1		Q				R2		W		T				(R1 + R2)	
	Ω	±	Ω^{-1}	±	N	±	Ω	±	Ω^{-1}	±	Ω^{-1}	±	$s^{1/2}$	±	Ω	±
Control 1	5.36	0.36	0.0296	0.0279	0.719	0.088	3.85	2.74	0.040	0.032	0.05	0.04	0.072	0.046	9.21	3.10
Control 2[a]	6.44	0.20	0.0253	0.0204	0.528	0.130	1.99	0.75	0.312	0.189	0.46	0.21	0.030	0.004	8.44	0.75
MEC[a]	7.76	2.07	0.0882	0.0004	0.783	0.013	1.14	0.62	0.218	0.081	0.22	0.01	0.173	0.048	8.89	2.07

[a] The EIS was performed after 6 months.

and cathode (Fig. 5). As depicted in Fig. 5 (a), there was a significant drop in the catalytic current associated with the oxidation of acetate by the bioanode after the tests, which is in agreement with the drop of current densities observed at such high voltages. The bioanode activity was clearly hindered which could be the result of toxic compounds being produced from abiotic oxidation. In addition, the anode potential reached 1.0 V when a 2.0 V cell voltage was applied, as can be seen in Fig. 2 (a). At such a high potential, water hydrolysis is likely to occur, thus leading to oxygen and hydroxides which are harmful to anaerobic bioanodes. However, Fig. 5 (b) shows that the biocathode maintained its catalytic activity. It can be observed from the figure that reduction activity became more important in the region below −0.9 V. Furthermore, small oxidation and reduction peaks can also be noted around −0.7 and −0.3 V in the biocathode compared to the control. It was previously reported that the oxidation peak is associated with the oxidation of hydrogen oxidation on the reverse scan of the hydrogen evolution reaction [9,10,19]. When a new CV scan was recorded in a smaller window between −0.8 and 0 V (data not shown) instead of −1.0 and 0 V (as in Fig. 5 (b)), the −0.7 V oxidation peak became insignificant. These redox features are attributed to the reversible catalytic activity of hydrogenase. On the other hand, the reduction peak is possibly due to non-hydrogen-producing activity and might be related to the formation of organic carbons such as acetate [9].

The growth of biofilms on the surface of the anode and cathode was analysed by electrochemical impedance spectroscopy (EIS). Fig. 5 (c) present the spectrograms recorded for the cell (between the anode and cathode).

The semicircle with a tail observed in the spectrograms can be explained with an electrochemical equivalent circuit called a Randles circuit [39–43]. The modified circuit and its simplified form are shown in Fig. 5 (d) and the coefficients from the fitted models are reported in Table 1. The former circuit represents both the anode and cathode in the cell while the latter is simplified by combining similar behaviour in both the anode and cathode to single elements [39,40]. The simplified circuit consisted of two resistances, R_1 and R_2, one constant phase element Q, and two diffusion properties W and T. R_1 represents the solution resistance and R_2 the charge transfer resistance which is related to the conductivity of solid materials in the cell. Q depicts the imperfect capacitance behaviour in the system. The imperfections are usually caused by the biofilm growth on the electrode surface and by the electrode material used in the system. Meanwhile W is the Warburg diffusion, and T is the finite diffusion coefficient which represents diffusion across the biofilm layers and porous electrodes [43].

As depicted in Fig. 5 (c), the semicircle representing the internal resistance of the cell is more apparent in the MEC than in the control and initial results, as layers of biofilm were actively growing and attaching onto the electrode's surface. Based on the results determined from the equivalent circuit in Fig. 5 (d), the internal resistances dropped from 9.21 Ω (Initial) to 8.44 Ω (Control) and 8.89 Ω. As presented in Table 1, the charge transfer resistance slightly decreased compared to the initial value, which can be attributed to the attachment of electrochemically active microbes on the

electrode, changing its surface morphology and electrochemical properties [19]. However, solution resistance decreased disproportionally to the charge transfer resistance. Depletion of reactants and accumulation of products in the solutions were probably the main factors affecting the solution properties and the resistance. In contrast, constant phase element impedance value increased due to the increase of the biofilm thickness and the accumulation of older layers. Meanwhile the tails of the spectrograms represent the diffusion behaviours W and T of the biofilms and porous electrodes. The angle of the tail remained slightly lower after the chronoamperometry test which means that the diffusion properties also slightly changed compared to the control and initial results [39–42].

Energy recovery and contribution

Fig. 6 presents the energy recovery, overall efficiency and energy contribution of this study. Based on Fig. 6 (a), the Coulombic efficiency R_{CE}, and substrate oxidation energy yield η_s, were determined based on the acetate removal at the anode. R_{CE} increased from 0% at 0.3 V to a peak value of 322% at 0.7 V before it dropped and reached a plateau of about 170% after 1.4 V. The cathodic recovery $R_{cat,}$ and external input energy yield η_e were calculated based on hydrogen detected at the cathode. R_{cat} increased slower than R_{CE} from 0% at 0.3 V to 57% at 1.0 V and remained constant after 0.5 V.

As can be seen in Fig. 6 (b), the trends of energy efficiencies η_e, η_s, and η_{e+s}were similar. However, η_s had the highest value compared to the other followed by η_e and η_{e+s}. All three efficiencies increased at 0.5 V and peaked at 1.0 V before decreasing until to 1.4 V to remain stable. A sudden drop at 2.0 V can also be noted in the figures due to the loss of the bioanode activity. Even though η_s was higher, overall efficiency, η_{s+e} was low as a result of low a η_e value. The best η_{s+e} that could be achieved in this study is 29.4% at 1.0 V applied voltage. The difference in efficiencies at the anode and cathode is related to the different bacterial communities involved at each electrode (e.g. electrogens vs. autotrophs) catalysing different reactions (oxidation vs. reduction) at different reaction rates (e.g. days vs. months). In addition, the consumption rate at the anode was higher than the production rate at the cathode. Another reason for the low efficiencies measured is the loss of energy to overpotentials due to system configuration and microbe's assimilation to maintain cell metabolism [2,36,44]. Energy efficiency from external power supply, η_e was recorded as low as 42.2% compared to that from the anode 97.3% indicating that the substrate oxidation might play a bigger part in the energy contribution [9,29,45]. However, since the calculations were based on the energy in the hydrogen produced (see Equations (4) and (5)), higher efficiency in η_s could be overestimated and low efficiency in η_e could be underestimated. The energy contribution from anode might be smaller than expected and vice versa. Since the current used to produce specific amount of hydrogen at the cathode was supplied by both anodic oxidation and external power, the determination of anode or cathode energy yield based on the total amount of hydrogen

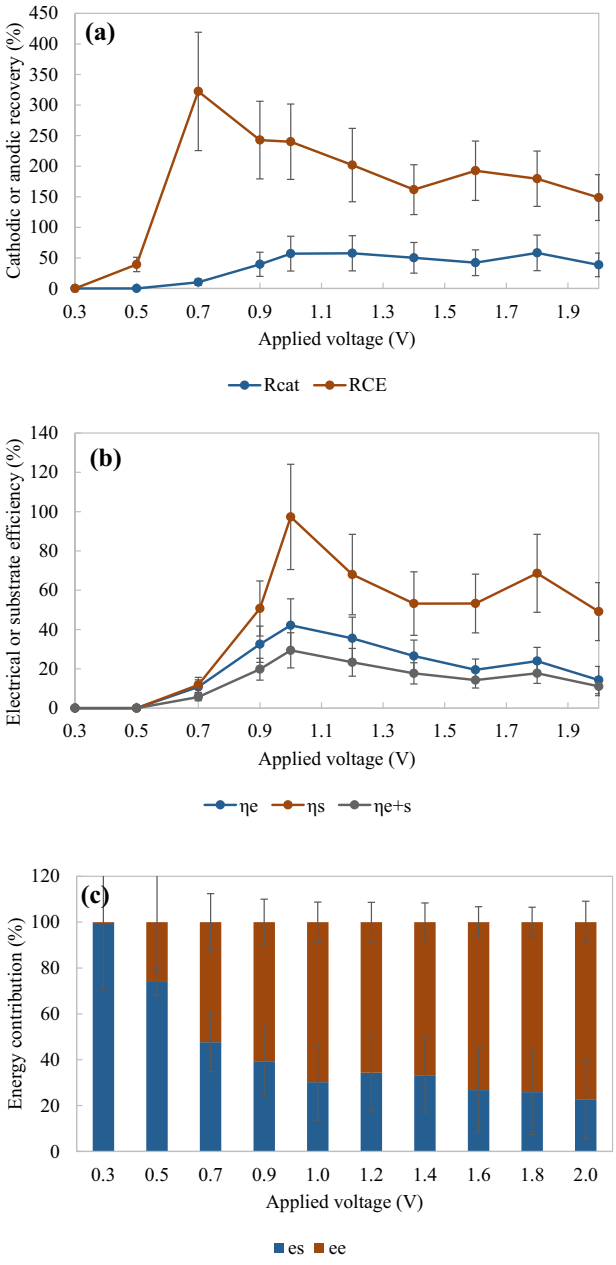

Fig. 6 – (a) Recovery yield, (b) energy efficiency and (c) energy contribution in the chronoamperometry test. Note: the recovery, efficiency and energy contribution were calculated based on hydrogen production in cathode and acetate consumption in anode. Note that the anodic or Coulombic efficiency, R_{CE} is more than 100% due to the calculation taking account of the total charge flow (using the current density) which includes part of the charges supplied from external power. The same estimation applies to substrate efficiency, η_s when only substrate oxidation energy is taken consideration relative to hydrogen energy production.

is not an accurate approach. Therefore, the overall energy yield η_{s+e} (see Equation (3)), was obtained because it is more accurate to estimate the efficiency of the whole system (combination of anode and cathode efficiencies).

Finally, Fig. 6 (c) shows an overview of the energy contribution (break down of the overall efficiency) from the acetate-oxidising bioanode (e_s) and the external power supply (e_e) when applied voltage increased from 0.3 to 2.0 V. The energy contribution from the oxidation of acetate was as high as 99.2% at 0.30 V, but it should also be kept in mind that at this potential the hydrogen production was very low. At the optimum hydrogen-producing applied voltage of 1.0 V, the energy contribution from the oxidation of acetate and external power supply were of 30.2% and 69.8% respectively, stressing out the importance of the bioanode to reduce the cost of external power supply. Finally, the contribution of the bioanode was only of 22.5% when the applied voltage reached 2.0 V, which is consistent with the progressive loss of its catalytic activity.

Conclusions

The impact of operational voltage on the performance of a microbial electrolysis cell for hydrogen production was studied. A minimum cell voltage of 0.3 V was sufficient to promote the growth of biofilms on both electrodes' surfaces. The bioanode was first developed after one week of operation and was important to provide lower potential for enriching biocathode. Chronoamperometry tests suggested that the biocathode growth was much slower than the bioanode based on both half-cell potentials and current evolutions. A window of applied voltage between 0.9 and 1.8 V was determined as the most relevant operational voltage to maintain the biocathode potential low enough for reduction reactions and at the same time protect the bioanode ability for oxidation reactions. The optimum applied voltage was determined as 1.0 V with a peak hydrogen production rate of nearly 6.0 L m^{-2} cathode day^{-1}. The shifts of pH and conductivity under the operational voltages could cause serious problems to the system especially harming the bioanode at low pH (accumulation of protons) and blocking the hydrogen production at high pH value (lack of protons) at the cathode. At the lowest applied voltage of 0.3 V, the anode contributed almost 99% of the total current measured. At the optimum applied voltage of 1.0 V, the bioanode contributed for almost 1/3 of the total energy used for the production of hydrogen, marking the importance of bioanode to reduce the cost associated with the utilisation of an external power supply.

Acknowledgments

This research was financially supported by EPSRC (EP/N009746/1), NERC (NE/L01422X/1), EPSRC Impact accelerate awards (IAA), and UKIERI Department of Science & Technology Partnerships (2014-15 S. No. 16). Swee Su Lim was sponsored by Skim Latihan Akademik IPTA (SLAI) under the Malaysian Ministry of Education (MoE).

Appendix A. Supplementary data

Supplementary data to this article can be found online at https://doi.org/10.1016/j.ijhydene.2019.11.142.

REFERENCES

[1] Ketep SF, Bergel A, Bertrand M, Achouak W, Fourest E. Lowering the applied potential during successive scratching/re-inoculation improves the performance of microbial anodes for microbial fuel cells. Bioresour Technol 2013;127:448–55.
[2] Kim KY, Chae KJ, Choi MJ, Ajayi FF, Jang A, Kim CW, et al. Enhanced Coulombic efficiency in glucose-fed microbial fuel cells by reducing metabolite electron losses using dual-anode electrodes. Bioresour Technol 2011;102:4144–9.
[3] Lim SS, Daud WRW, Md Jahim J, Ghasemi M, Chong PS, Ismail M. Sulfonated poly(ether ether ketone)/poly(ether sulfone) composite membranes as an alternative proton exchange membrane in microbial fuel cells. Int J Hydrogen Energy 2012;37:11409–24.
[4] Spurr MWA. Microbial fuel cell-based biosensors for estimation of biochemical oxygen demand and detection of toxicity. UK: Newcastle University; 2016. Unpublished manuscript.
[5] Wang X, Feng Y, Ren N, Wang H, Lee H, Li N, et al. Accelerated start-up of two-chambered microbial fuel cells: effect of anodic positive poised potential. Electrochim Acta 2009;54:1109–14.
[6] Zhu X, Tokash JC, Hong Y, Logan BE. Controlling the occurrence of power overshoot by adapting microbial fuel cells to high anode potentials. Bioelectrochemistry 2013;90:30–5.
[7] Bajracharya S, ElMekawy A, Srikanth S, Pant D. Cathodes for microbial fuel cells. In: Scott KY, Eileen Hao, editors. Microbial electrochemical and fuel cells. Boston: Woodhead Publishing; 2016. p. 179–213.
[8] Zhen G, Lu X, Kumar G, Bakonyi P, Xu K, Zhao Y. Microbial electrolysis cell platform for simultaneous waste biorefinery and clean electrofuels generation: current situation, challenges and future perspectives. Prog Energy Combust Sci 2017;63:119–45.
[9] Lim SS, Yu EH, Daud WRW, Kim BH, Scott K. Bioanode as a limiting factor to biocathode performance in microbial electrolysis cells. Bioresour Technol 2017;238:313–24.
[10] Batlle-Vilanova P, Puig S, Gonzalez-Olmos R, Vilajeliu-Pons A, Bañeras L, Balaguer MD, et al. Assessment of biotic and abiotic graphite cathodes for hydrogen production in microbial electrolysis cells. Int J Hydrogen Energy 2014;39:1297–305.
[11] Jourdin L, Raes SMT, Buisman CJN, Strik DPBTB. Critical biofilm growth throughout unmodified carbon felts allows continuous bioelectrochemical chain elongation from CO2 up to caproate at high current density. Frontiers in Energy Research 2018;6.
[12] Raes SMT, Jourdin L, Buisman CJN, Strik DPBTB. Continuous long-term bioelectrochemical chain elongation to butyrate. ChemElectroChem 2017;4:386–95.
[13] Zaybak Z, Pisciotta JM, Tokash JC, Logan BE. Enhanced start-up of anaerobic facultatively autotrophic biocathodes in bioelectrochemical systems. J Biotechnol 2013;168:478–85.
[14] Vassilev I, Ledezma P, Freguia S, Kromer JO, Keller J, Virdis B. Microbial electrosynthesis: microbes turning CO2 into volatile fatty acids and associated alcohols. In: General

meeting of the international society for microbial electrochemistry and Technology. Lisbon, Portugal: ISMET 2017; 2017. p. 75.
[15] Choi O, Sang B-I. Extracellular electron transfer from cathode to microbes: application for biofuel production. Biotechnol Biofuels 2016;9:11–25.
[16] Rabaey K, Rozendal RA. Microbial electrosynthesis — revisiting the electrical route for microbial production. Nat Rev Microbiol 2010;8:706–16.
[17] Rozendal RA, Jeremiasse AW, Hamelers HVM, Buisman CJN. Hydrogen production with a microbial biocathode. Environ Sci Technol 2008;42:629–34.
[18] Jeremiasse AW, Hamelers HVM, Buisman CJN. Microbial electrolysis cell with a microbial biocathode. Bioelectrochemistry 2010;78:39–43.
[19] Aulenta F, Catapano L, Snip L, Villano M, Majone M. Linking bacterial metabolism to graphite cathodes: electrochemical insights into the H2-producing capability of desulfovibrio sp. ChemSusChem 2012;5:1080–5.
[20] Geelhoed JS, Hamelers HVM, Stams AJM. Electricity-mediated biological hydrogen production. Curr Opin Microbiol 2010;13:307–15.
[21] Lim SS, Kim BH, Li D, Feng Y, Daud WRW, Scott K, et al. Effects of applied potential and reactants to hydrogen-producing biocathode in a microbial electrolysis cell. Frontiers in Chemistry 2018;6:318.
[22] Escapa A, Mateos R, Martínez EJ, Blanes J. Microbial electrolysis cells: an emerging technology for wastewater treatment and energy recovery. From laboratory to pilot plant and beyond. Renew Sustain Energy Rev 2016;55:942–56.
[23] Kadier A, Simayi Y, Abdeshahian P, Azman NF, Chandrasekhar K, Kalil MS. A comprehensive review of microbial electrolysis cells (MEC) reactor designs and configurations for sustainable hydrogen gas production. Alexandria Engineering Journal 2016;55:427–43.
[24] Kumar G, Bakonyi P, Zhen G, Sivagurunathan P, Koók L, Kim S-H, et al. Microbial electrochemical systems for sustainable biohydrogen production: surveying the experiences from a start-up viewpoint. Renew Sustain Energy Rev 2017;70:589–97.
[25] Coma M, Puig S, Pous N, Balaguer MD, Colprim J. Biocatalysed sulphate removal in a BES cathode. Bioresour Technol 2013;130:218–23.
[26] Luo H, Fu S, Liu G, Zhang R, Bai Y, Luo X. Autotrophic biocathode for high efficient sulfate reduction in microbial electrolysis cells. Bioresour Technol 2014;167:462–8.
[27] Bond DR, Lovley DR. Electricity production by Geobacter sulfurreducens attached to electrodes. Appl Environ Microbiol 2003;69:1548–55.
[28] Logan BE, Hamelers B, Rozendal R, Schröder U, Keller J, Freguia S, et al. Microbial fuel Cells: methodology and technology. Environ Sci Technol 2006;40:5181–92.
[29] Call D, Logan BE. Hydrogen production in a single chamber microbial electrolysis cell lacking a membrane. Environ Sci Technol 2008;42:3401–6.
[30] Bajracharya S, Yuliasni R, Vanbroekhoven K, Buisman CJN, Strik DPBTB, Pant D. Long-term operation of microbial electrosynthesis cell reducing CO2 to multi-carbon chemicals with a mixed culture avoiding methanogenesis. Bioelectrochemistry 2017;113:26–34.
[31] Jourdin L, Freguia S, Donose BC, Keller J. Autotrophic hydrogen-producing biofilm growth sustained by a cathode as the sole electron and energy source. Bioelectrochemistry 2015;102:56–63.
[32] Mohanakrishna G, Seelam JS, Vanbroekhoven K, Pant D. An enriched electroactive homoacetogenic biocathode for the microbial electrosynthesis of acetate through carbon dioxide reduction. Faraday Discuss 2015;183:445–62.
[33] Kim BH, Park HS, Kim HJ, Kim GT, Chang IS, Lee J, et al. Enrichment of microbial community generating electricity using a fuel-cell-type electrochemical cell. Appl Microbiol Biotechnol 2004;63:672–81.
[34] Jeremiasse AW, Hamelers HVM, Croese E, Buisman CJN. Acetate enhances startup of a H2-producing microbial biocathode. Biotechnol Bioeng 2012;109:657–64.
[35] LaBelle EV, Marshall CW, Gilbert JA, May HD. Influence of acidic pH on hydrogen and acetate production by an electrosynthetic microbiome. PLoS One 2014;9. e109935.
[36] Kim BH, Lim SS, Daud WRW, Gadd GM, Chang IS. The biocathode of microbial electrochemical systems and microbially-influenced corrosion. Bioresour Technol 2015;190:395–401.
[37] van Eerten-Jansen MCAA, Jansen NC, Plugge CM, de Wilde V, Buisman CJN, ter Heijne A. Analysis of the mechanisms of bioelectrochemical methane production by mixed cultures. J Chem Technol Biotechnol 2015;90:963–70.
[38] Foad Marashi SK, Kariminia H-R. Performance of a single chamber microbial fuel cell at different organic loads and pH values using purified terephthalic acid wastewater. J Environ Health Sci Eng 2015;13:27–33.
[39] Dominguez-Benetton X, Sevda S, Vanbroekhoven K, Pant D. The accurate use of impedance analysis for the study of microbial electrochemical systems. Chem Soc Rev 2012;41:7228–46.
[40] Sekar N, Ramasamy RP. Electrochemical impedance spectroscopy for microbial fuel cell characterization. J Microb Biochem Technol 2013. S6:004.
[41] Borole AP, Aaron D, Hamilton CY, Tsouris C. Understanding long-term changes in microbial fuel cell performance using electrochemical impedance spectroscopy. Environ Sci Technol 2010;44:2740–5.
[42] He Z, Mansfeld F. Exploring the use of electrochemical impedance spectroscopy (EIS) in microbial fuel cell studies. Energy Environ Sci 2009;2:215–9.
[43] Macdonald DD. Reflections on the history of electrochemical impedance spectroscopy. Electrochim Acta 2006;51:1376–88.
[44] Nimje VR, Chen C-C, Chen H-R, Chen C-Y, Tseng M-J, Cheng K-C, et al. A single-chamber microbial fuel cell without an air cathode. Int J Mol Sci 2012;13:3933–48.
[45] Logan BE, Call D, Cheng S, Hamelers HVM, Sleutels THJA, Jeremiasse AW, et al. Microbial electrolysis cells for high yield hydrogen gas production from organic matter. Environ Sci Technol 2008;42:8630–40.